Supporting Information

Combining in situ NEXAFS spectroscopy and CO_2 methanation kinetics to study Pt and Co nanoparticle catalysts reveals key insights into the role of platinum in promoted cobalt catalysis.

Simon K. Beaumont,[‡a,b,c] Selim Alayoglu,[‡a,b] Colin Specht,[a,b] William D. Michalak,[a,b] Vladimir V. Pushkarev, [† a,b] Jinghua Guo,[d,e] Norbert Kruse,[f,g] Gabor A. Somorjai*[a,b]

[a] Department of Chemistry, University of California, Berkeley, CA; [b] Materials Sciences Division, Lawrence Berkeley National Laboratory, Berkeley, CA; [c] Department of Chemistry, Durham University, South Road, Durham, DH1 3LE, United Kingdom; [d]Advanced Light Source, Lawrence Berkeley National Laboratory, Berkeley CA; [e] Department of Chemistry and Biochemistry, University of California, Santa Cruz, CA; [f] Université Libre de Bruxelles, Chimie Physique des Matériaux, Campus de la Plaine CP 243,B-1050 Bruxelles, Belgium. [g]Department of Chemical Engineering and Bioengineering, Washington State University, Pullman, WA.

1. Experimental Methodology

Nanoparticle and catalyst synthesis:

10 nm Cobalt nanoparticles, 1.9 nm Pt nanoparticles and Co-Pt bimetallic samples were prepared as reported previously.'[1,2,3]

12 nm Platinum nanoparticles were prepared by an injection of $Pt(acac)_2$ precursor salt in 1-dodecanol into a hot solution of oleic acid in 1-dodecanol at 230 °C. Typically, 20 mg $Pt(acac)_2$ (Aldrich, 99.9% pure) was dissolved in 3 mL 1- dodecanol (Aldrich, ACS grade) in a 20 mL scintillation vial. 150 µL oleic acid (Aldrich technical grade) was dissolved in 10 mL 1-dodecanol in a 50 mL three-neck round bottom flask. The flask was evacuated and flushed with Ar several times, and then placed in an oil bath pre-heated to 230 °C. The temperature was monitored with an internal K-type thermocouple. When the temperature reached the set point, the Pt precursor solution was injected into the hot oleic acid solution. The reaction was allowed to run for 20 min. The reaction was terminated by removing the flask from the oil bath and the flask was cooled down by using a cold air blower. Acetone (VWR reagent grade) was poured into the colloidal suspension, and the mixture was centrifuged at 4300 rpm for 10 min. The precipitate was then redispersed in chloroform (VWR reagent grade) for further use.

All nanoparticles were subsequently supported in mesoporous silica, MCF-17, which had been synthesized according to the reported method,[4] and dried at 200 °C under vacuum prior to use. MCF-17 mesoporous silica, with pore sizes in the characteristic range of 20–50 nm, was deliberately selected to accommodate the relatively large nanoparticles (9 - 13 nm). MCF-17 was then dispersed in chloroform before adding the required volume of nanoparticle solution(s), also sonicated to ensure redispersion in the chloroform in which they were stored. Sonication was continued for 40 min before the suspension was centrifuged at 3000 rpm and washed with 20 vol. % ethanol in acetone seven times. The supported catalyst was then oven dried at 100 °C. Supported nanoparticle catalysts were conditioned at 450 °C in 1 atm. H_2 (80% in Helium) in the reactor prior to catalytic testing. (This temperature was empirically found to be optimal in terms of resultant activity and is believed to correspond to the best conditions for removal of the organic material which remains from the synthesis without significant sintering.)

Nanoparticle characterisation:

TEM and HRTEM images were obtained by using Jeol 2100 LaB_6 transmission electron microscope. 2-D nanoparticle films were characterized by using a ZEISS Ultra55 analytical scanning electron microscope. STEM/EDS analysis was carried out by using a Jeol 2100F transmission electron microscope equipped with an INCA energy dispersive spectrometer. Elemental maps of the Pt L, Co K and Si K spectral lines were obtained in the scanning mode by using a 1.5 nm e-beam probe. X-ray photoelectron spectra of 2-D nanoparticle films were taken at 10^{-8} Torr base pressure by using a Perkin Elmer PHI 5400 spectrometer with an Al K source.

ICP-AES analysis was conducted with an ICP Optima 7000 DV instrument. The Co emission line at 238.175 nm and Pt emission line 204.937 nm were employed for the calibration and measurements. For this, 10-20 mg charges of MCF-17 supported nanoparticle catalyst samples were first dissolved in 3 mL aqua regia. The residual solid was filtrated by centrifugation and the solution was diluted to 50 mL with MilliQ water to be analyzed in

ICP-AES. The calibration standards were prepared from a Co ICP standard (Aldrich, 2 wt. % in nitric acid) and a Pt ICP standard (Aldrich, 5 wt. % in hydrochloric acid) in 6 vol. % aqua regia. The determined metal loading for each catalyst sample is given below.

Catalytic reaction measurements:

Kinetic studies were performed using a steel tubular plug flow reactor (i.d. 3 mm) heated using a purpose built PID-controlled electrical furnace. The catalyst sample (50 mg) was retained between plugs of quartz wool, and the reactor temperature monitored with a K-type thermocouple. A reactant gas feed consisting of CO_2 (11.1 sccm, BOC 99.5%), H_2 (33.3 sccm, Praxair 99.999%) balanced with He (5.6 sccm, Praxair 99.999%), corresponding to the 1:3 reaction stoichiometry, was delivered via a series of independent calibrated mass flow controllers (MKS Instruments). The total flow was 50 sccm, giving a gas hourly space velocity ([cm^3 (STP) (H_2 + CO_2 + He)/g supported catalyst]/time) of 60,000 h^{-1}. The pressure (as monitored by a capacitance gauge at the exit to the reactor) was regulated via a needle valve to 6 bar or opened fully to allow atmospheric pressure (1 bar) measurements. The gases exiting the reactor were analyzed using a Hewlett Packard HP 5890 Series II chromatograph equipped with both FID and TCD detectors. Hayasep-D packed columns were employed for both the chromatographic separation of CO_2, CO, and CH_4 (TCD) and detecting the presence of C_1–C_3 hydrocarbons (FID). Calibration of retention times and peak intensities was made directly with all observed reactants and products. Under these conditions CO_2 conversions were typically ~5 %, minimizing the contribution of subsequent reactions of the primary products with the catalyst. The TOF values provided are derived by taking the projected surface area based on TEM cobalt particle size, the weight % cobalt loading arrived at from ICP-AES, and the number of product molecules produced as monitored by GC. This results in a lower bound on TOF, since it assumes all the surface of the Co particles is available to the reactants. Errors for TOF values are derived from the standard deviation of duplicate runs. Only Co surface is considered as we previously identified pure Pt particles do not produce methane under these conditions. For the bimetallic CoPt particles, the TOF is calculated assuming 50% of the surface area is occupied by Co atoms, however given the inactivity of this material for CO_2 to methane conversion reported on previously the exact method of calculation is of little consequence.[2] Carbon balance for these reactions indicates that little loss of carbon / carbon deposition occurs (non-detectable). Since the focus is using model catalysts to explore how changing the combination of Co and Pt affects reaction rate, initial reaction rate measurements were performed over the first 5 h after catalyst pre-treatment. It should be noted we have previously found no significant deactivation (<10%) in the rate of 10 nm Co catalysts over 24 hours at 6 bar and 300 °C (more severe than used presently) and also explored whether significant morphology / size changes occur as a result of either pre-treatment or reaction and found that they do not.[3]

In situ NEXAFS spectroscopy:

In situ NEXAFS spectroscopy measurements were conducted at beamline 7.0.1 (now moved to 8.0.1) at the Advanced Light Source synchrotron radiation facility at Lawrence Berkeley National Laboratory. Samples were prepared as single layer films of nanoparticles (~50% coverage) by dip-coating onto a Silicon wafer. For samples with platinum and cobalt nanoparticles, a Si wafer was dipped into first a dilute Pt colloidal suspension (~5 μmol/mL chloroform) and then a concentrated Co colloidal suspension (~0.3 mmol/mL chloroform). As indicated by the SEM images (see below), Pt and Co nanoparticles exist in separate domains with no apparent physical overlap between the two systems. The Pt:Co ratios are very roughly 1:30 for the 12 nm Pt, determined from the SEM pictures, and 1:15 for the 1.9 nm Pt, determined from the XPS spectrum (as described below). Since it acts as the closest feasible model for the SiO_2 supported 3-D catalyst and is found to be still sufficiently conducting, the native oxide layer was not removed prior to nanoparticle deposition. NEXAFS spectroscopy studies were carried out in our purpose-built flow cell as described elsewhere.[5] X-ray absorption at the Co L-edge was recorded with 0.3 eV resolution using the total electron yield signal measured by monitoring the flow of electrons from earth to the sample. Reducibility of each sample was studied by first oxidizing in an atmospheric pressure flow of O_2 (Praxair, 99.993%) in He (Airgas, 99.9999%) (1:4) at 100 °C, cooling and then incrementing the temperature recording a series of Co L-edge spectra at each temperature (over a time scale of 40 - 80 minutes) in 1 bar pure H_2 (Praxair, 99.996%) until no further changes between spectra were observed. This was done to ensure the Co had arrived at a stable state or was only changing very slowly on the timescale of the reduction process. Spectra were fitted to step edge normalized reference data acquired previously at the same beamline in vacuum via a least squares fitting method. Since it is the peak shape around the L_3-edge that changes most dramatically between different oxidation states, the spectra were fitted between 785 eV and 780 eV to minimize the impact of background and normalization errors that may be present across the whole spectrum and become a larger percentage of the overall fit if larger regions of the spectra at higher photon energies are included. Full results for the fitting of all spectra and an example showing various components and the results fit are provided below.

2. Fitting of NEXAFS spectra:

Table S1. **Summary of fitting results for all spectra in main text Figures 3 and 4.**

Sample	Conditions	% Co(0)	% Co(II) (O_h)	% Co(II) (T_d)	Co_3O_4
10 nm Co alone	oxidised, RT	13	73	14	0
	80 °C, H_2	5	48	46	0
	175 °C, H_2	42	45	13	0
	225 °C, H_2	73	27	0	0
10 nm Co + 12 nm Pt	oxidised, RT	0	55	0	45
	80 °C, H_2	22	77	1	0
	175 °C, H_2	58	21	17	4
	225 °C, H_2	87	13	0	0
10 nm Co + 1.9 nm Pt	oxidised, RT	13	78	9	0
	80 °C, H_2	41	59	0	0
	175 °C, H_2	72	28	0	0
	225 °C, H_2	89	7	4	0

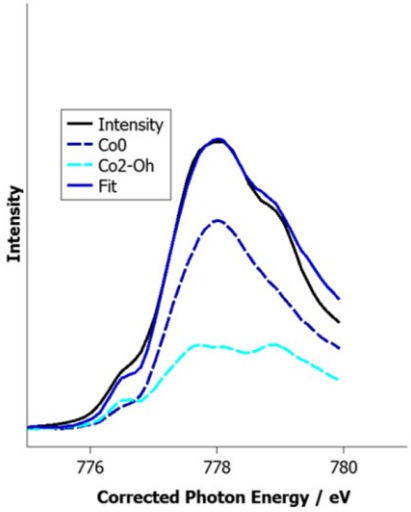

Figure S1. Example of fit of Co L_3-edge NEXAFS spectrum using least squares fitting of Co reference spectra: Co with 1.9 nm Pt in H_2 at 175 °C. Reference data: Co0 metallic cobalt; Co2-Oh oxidation state 2+ cobalt reference with cobalt atoms octahedrally co-ordinated.

3. Ex situ characterisation of NEXAFS samples:

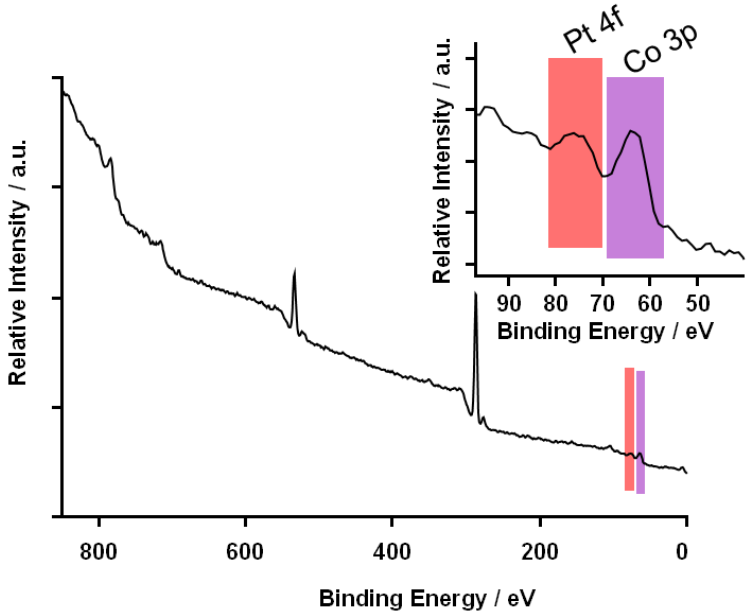

Figure S2. XP Spectrum of Si wafer supported NEXAFS sample (~1.9 nm Pt with 10 nm Co), from which an approximate Co:Pt ratio was estimated as described below. Inset shows Pt 4f and Co 3p region.

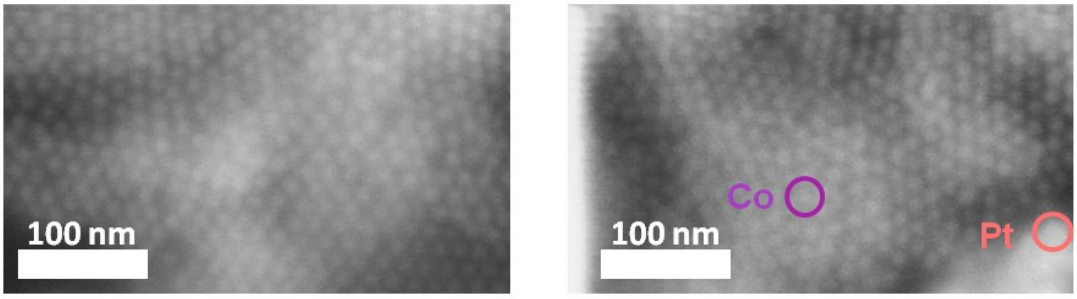

Figure S3. Examples of pre-NEXAFS sample (~12 nm Pt with 10 nm Co), from which a very rough Co:Pt ratio was estimated as described below.

Estimation of Pt:Co ratios for NEXAFS samples:

Samples comprising ~1.9 nm Pt with 10 nm Co particles: the Pt to Co atomic ratio was determined using XPS. The spectrum shown in Figure S2 indicates a trace Pt signal, which (given the much larger X-ray cross section area of Pt vs Co when using Al K incident photons) equates to an atomic ratio for Co:Pt of ~ 15 : 1.

Samples comprising ~12 nm Pt with 10 nm Co particles: XPS analysis of this sample did not detect Pt, so we anticipate less Pt than the 1.9 nm Pt particle-containing sample. Instead, a crude estimate of the amount of Pt was obtained using a series of SEM images (examples in Figure S3), based on size and contrast in the electron image (making use of the Z-sensitive backscattering contribution and variations in contrast). Example Pt and Co particles are highlighted, but are best seen by varying the contrast in the images. The number ratio is estimated to be ~ 1:37 Pt : Co particles (based on counting ~ 2000 particles). By accounting for the average particle sizes (known from TEM), assuming an fcc crystal packing structure and lattice constants of 3.51 Å and 3.92 Å for Co and Pt respectively, gives a Pt:Co atomic ratio of ~ 1:30. While this method is only very approximate, the determined ratio is in good agreement with our expectations for this sample based on the difference in the XP spectra. Moreover, the amount of Pt present still has an impact on the relative extent of reduction of the cobalt as monitored by NEXAFS. X-ray fluorescence or EELS could not be used satisfactorily with these samples as a dense / close packed layer is required for NEXAFS in order to obtain signal, and this means that even with the smallest probe

sizes commonly available in EDS-SEM imaging (which are large than for TEM), there is significant overlap with a number of nanoparticles.

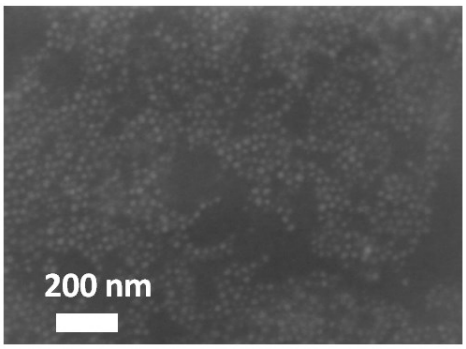

Figure S4. Example of a post-NEXAFS sample (1.9 nm Pt with 10 nm Co), which appears to show no (little visible) damage / change from the expected structure has occurred during spectral acquisition.

4. Estimation of surface atomic layer fraction of the NEXAFS signal when probing a 10 nm nanoparticle.

It is assumed that particles being probed have10 nm diameters and the surface layer is 0.27 nm (twice the empirical atomic radius of a Co atom). The reported probing depth of the technique is ~ 2.7 nm.[6] To estimate the surface atomic layer fraction of NEXAFS signal we assume an exponential decay in resultant signal intensity from the surface of the particle as

$$relative\ intensity \propto e^{-(5-r)/2.7}$$

where *r* is the distance from the centre of the particle. The relative intensity may be integrated for the surface shell of a sphere and the whole particle using:

$$\int_0^5 e^{-(5-r)/2.7} \cdot r^2 dr \quad \text{and} \quad \int_{4.73}^5 e^{-(5-r)/2.7} \cdot r^2 dr$$

The ratio of these integrals implies that approximately 22% of the NEXAFS signal (as a very crude approximation) should be originating from the surface layer (ignoring the distribution of sizes, particle shape and probing direction).

5. ICP-AES results.

Table S2: **Loading of Co and Pt in each MCF-17 supported catalyst sample determined from ICP-AES.**

Sample	wt % Co	wt % Pt
10 nm Co alone / MCF-17	4.9	0.0
11nm CoPt bimetallic / MCF-17	2.7	6.9
10 nm Co + 12 nm Pt / MCF-17	4.0	0.7

6. Ex situ characterization using STEM/EDS of Pt and Co particle mixture after deposition on 3D mesoporous silica.

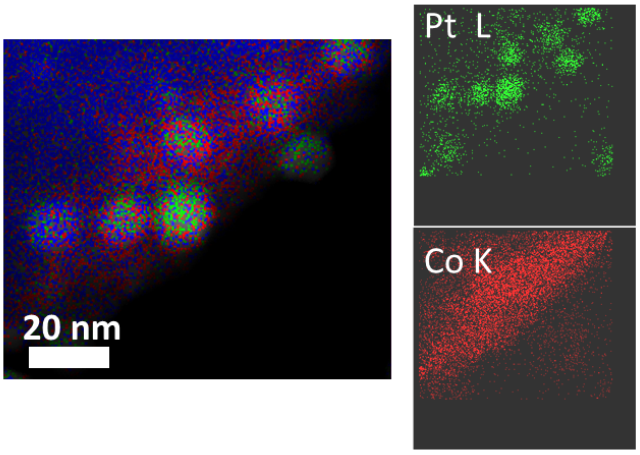

Figure S5. Example of STEM-EDS phase mapping of 10 nm Co + 12 nm Pt / MCF-17 3-D sample, showing Pt particles (green) and presence of cobalt (red), on silica (blue).

Discussion of STEM-EDS: Although identifiable Pt features of the correct size can be seen using the EDS technique as a local chemical probe (Figure S5), the overall higher concentration of cobalt nanoparticles, and the 3-D nature of these materials, makes identification of specific cobalt particles impossible when summed over the vertical height of these thick 3-D samples such that multiple particles are likely to be probed. ICP-AES is therefore the best measure of particle densities within the 3-D samples.

7. References:

1 Kuhn, J. N.; Tsung, C.-K.; Huang, W.; Somorjai, G. A. *J. Catal.* **2009**, *265*, 209.
[2] Alayoglu, S.; Beaumont, S. K.; Zheng, F.; Pushkarev, V. V.; Zheng, H. M.; Iablokov, V.; Liu, Z.; Guo, J. H.; Kruse, N.; Somorjai, G. A. *Top. Catal.* **2011**, *54*, 778.
[3] Iablokov, V.; Beaumont, S. K.; Alayoglu, S.; Pushkarev, V. V.; Specht, C.; Gao, J. H.; Alivisatos, A. P.; Kruse, N.; Somorjai, G. A. *Nano Lett.* **2012**, *12*, 3091
4 Schmidt-Winkel, P.; Lukens, W. W.; Yang, P.; Margolese, D. I.; Lettow, J. S.; Ying, J. Y.; Stucky, G. D. *Chem. Mater.* **2000**, *12*, 686.
5 Zheng, F.; Alayoglu, S.; Guo, J.; Pushkarev, V.; Li, Y.; Glans, P.-A.; Chen, J.-l.; Somorjai, G. *Nano Lett.* **2011**, *11*, 847.
[6] Akgül, G.; Aksoy, F.; Bozduman, A.; Ozkendir, O. M.; Ufuktepe, Y.; Lüning, J. Thin Solid Films **2008**, *517*, 1000.